Published in final edited form as:
Nano Lett. 2008 November ; 8(11): 3702–3708. doi:10.1021/nl8019328.

Factors governing helix formation in peptides confined to carbon nanotubes

Edward P. O'Brien[1,2], **George Stan**[3], **D. Thirumalai**[1,4,*], and **Bernard R. Brooks**[2]

1*Biophysics Program, Institute for Physical Science and Technology, University of Maryland, College Park, MD 20742*

2*Laboratory of Computational Biology, National Heart Lung and Blood Institute, National Institutes of Health, Bethesda, MD 20892*

3*Department of Chemistry, University of Cincinnati, Cincinnati, OH 45221*

4*Department of Chemistry and Biochemistry, University of Maryland, College Park, MD 20742*

Abstract

The effect of confinement on the stability and dynamics of peptides and proteins is relevant in the context of a number of problems in biology and biotechnology. We have examined the stability of different helix-forming sequences upon confinement to a carbon nanotube using Langevin dynamics simulations of a coarse-grained representation of the polypeptide chain. We show that the interplay of several factors that include sequence, solvent conditions, strength (λ) of nanotube-peptide interactions, and the nanotube diameter (D) determines confinement-induced stability of helicies. In agreement with predictions based on polymer theory, the helical state is entropically stabilized for all sequences when the interaction between the peptide and the nanotube is weakly hydrophobic and D is small. However, there is a *strong* sequence dependence as the strength of the λ increases. For an amphiphilic sequence, the helical stability increases with λ, whereas for polyalanine the diagram of states is a complex function of λ and D. In addition, decreasing the size of the 'hydrophobic patch' lining the nanotube, which mimics the chemical heterogeneity of the ribosome tunnel, increases the helical stability of the polyalanine sequence. Our results provide a framework for interpreting a number of experiments involving the structure formation of peptides in the ribosome tunnel as well as transport of biopolymers across nanotubes.

Introduction

There is great interest in studying protein folding and dynamics in confined spaces because of their possible relevance to a variety of biological problems [1-7]. These include the fate of newly synthesized proteins as they exit the nearly 100 Å long and approximately cylindrical ribosome tunnel [1,4], the effect of encapsulation of substrate proteins in the central cavity of the chaperonin GroEL [3], and the translocation of peptides across pores [8-11]. Understanding the factors that determine the stability of confined proteins is also relevant in biotechnology applications [12]. The effect of being localized in the cylindrical tunnel of the ribosome, or the GroEL cavity, on peptide and protein stability is hard to predict because of the interplay of a number of energy and length scales [13-21]. They include the decrease, with respect to bulk, in conformational entropy of the ensemble of unfolded and native states, and the residue-dependent solvent-averaged interaction between the substrate protein with the interior of the

*Corresponding author: Institute for Physical Science and Technology, University of Maryland, College Park, MD 20742, phone: 301-405-4803; fax: 301-314-9404; e-mail: thirum@glue.umd.edu.

confining pore. For example, the ribosome tunnel is lined with RNA near the peptidyl transfer center (PTC), and proteins closer to the the exit tunnel. As a result, the interaction of a nascent peptide with the walls of the tunnel varies as it traverses from the PTC towards the exit [6]. Thus, the formation of α-helical structure in the tunnel, that is observed in experiments [4], not only depends on the sequence but also on where the peptide is localized inside the ribosome [4,7].

A number of factors contribute to the changes in the stability of a peptide upon confinement to a nanotube. The simplest scenario is the entropic stabilization mechanism (ESM) [13-15, 22], which postulates that in confined spaces the number of allowed conformations is restricted compared to the bulk. As a result, the free energy change ΔF_U of the denatured state ensemble (DSE) and the ΔF_N in the native state ensemble (NSE) both increase. If the native state is not significantly altered in the confined space then $\Delta F_U \gg \Delta F_N$. Hence, confinement entropically stabilizes the native state relative to the DSE. The stabilization of polypeptide chains suggested by ESM holds good only when *D*, the diameter of the nanotube, exceeds a threshold value, because the entropy cost of confinement of the ordered (α-helical) conformation is prohibitive when *D* is small [17]. If water mediated interactions involving proteins are altered by confinement then it may be possible for $\Delta F_N > \Delta F_U$ [2,15,18,20,23]. In this case, the native state can be destabilized in nanotubes. More generally, if specific interactions between the polypeptide and the walls of the pore are relevant, as appears to be the case in certain regions of the ribosome tunnel, the diagram of states of a confined polypeptide or protein can be rich [24].

Here, we study the changes in stabilities of a number of peptide sequences that form helices to varying extents in bulk. By varying *D*, the strength of interaction, λ (see Eq. 7 in the SI), between the hydrophobic residues and the carbon nanotube, and the polypeptide sequence we show that an interplay of a number of factors determines the stability of helical states of peptides confined to nanotubes. We find that the helix is entropically stabilized when *D* is small and the interaction between peptides and nanotube is weak. As λ increases the peptide can adsorb onto the wall of the nanotube. Interestingly, adsorption results in stabilization of the helix for an amphiphilic sequence, and destabilization for a polyalanine sequence. If the wall of the nanotube is decorated with patches that are 'hydrophobic' the helical stability can increase for the polyalanine. Thus, a very rich diagram of states of helix forming sequences is envisioned upon confinement in a nanotube.

Methods

In order to explore a wide range of possibilities we consider several helix forming sequences. The sequences are GDLDDLLKKLKDLLKG (an amphiphilic sequence denoted by *AS*) [25, 26], polyasparagine N_{16} (a polar sequence denoted PN) [27,28], and polyalanine A_{16} (a hydrophobic sequence denoted PA) [29]. Each sequence is 16 residues long, which is close to the average helix length of ~14 found in globular proteins [30]. We use three variations of *AS* to probe the effects of varying the bulk peptide properties (the nature of the DSE and NSE) on confinement. The parameters of sequence AS_1 (see Table I) renders the helical state unstable in the bulk ($D \to \infty$). Sequences AS_2 and AS_3 are modeled so that they form stable helices in the bulk. The changes in the intra-peptide interactions (see Table I and SI for details) between the hydrophobic residues in AS_2 and AS_3 accounts for differences in ϵ_{BB} (Eq. 6 in SI) that can arise by adding cosolvents (see SI for details).

We use the Honeycutt-Thirumalai (HT) [31] model for the polypeptide chain. In the HT model, each amino-acid is represented by one bead located at the C_α-carbon position. A three letter code is used to classify the twenty naturally occurring amino acids; L for hydrophilic residues, B for hydrophobic residues, and N for neutral residues. The potential energy of a conformation

of a polypeptide with M residues, and coordinates $r_i(i = 1, 2, \ldots, M)$ in the HT representation is $V = V_B + V_A + V_D + V_{NB} + V_{HB}$, where V_B, V_A, and V_D are the bond-stretch, bond-angle, and the dihedral potentials respectively. The stability of the helices in the bulk can be altered by tuning the interaction, V_{NB}, between non-covalently linked beads, as well as the hydrogen bond potential V_{HB}. Details on the functional form, and the parameters of the energy function are provided in the Supplementary Information (SI).

In order to enhance the sampling of the conformational space of the peptide we use under-damped Langevin dynamics [32] with a friction coefficient of 0.016 ps^{-1}, and an integration time-step of 15 fs. Simulations are prepared and simulated in the NVT ensemble at 300 K using the CHARMM software package (version c32b2) [33].

Helical basin (HB)

A given peptide conformation is classified as helical using two order parameters. They are the end-to-end distance (R_{ee}), and the number of helical triads (N_{HT}). We define helical triads as three consecutive dihedral angles that are in the helical region ($35° \leq \phi \leq 75°$). A polypeptide with 16 residues has a total of eleven helical triads. In a completely helical conformation $N_{HT} = 11$, while $N_{HT} = 0$ corresponds to a completely random coil conformation. A conformation is deemed to be in the HB if 21.25 Å $< R_{ee} <$ 28.75 Å and $8 \leq N_{HT} \leq 11$. The two order parameters R_{ee} and N_{HT} separate the helical and denatured basins into distinct regions (see the inset in Fig. 1C).

Results and Discussion

For sequence AS_1 the probability of being in the HB (P_{HB}) is 0.17 in bulk. The values of P_{HB} for AS_2, AS_3, PA, and PN, are between 0.40-0.50 in the bulk (Table I).

Helices are entropically stabilized in narrow and weakly hydrophobic nanotubes

If the attractive interaction between the hydrophobic residues and the nanotube is weak ($\lambda <$ 0.4) then confinement enhances helix stability of all sequences provided $D < D^*$, where D^* depends on the sequence (Fig. 1) and is greater than or equal to 20 Å for the sequences studied here. For example, when AS_3, PA and PN are in a nanotube with D = 14.9 Å and λ = 0.01, the helix is stabilized by 0.71, 0.68 and 0.49 kcal/mol, respectively (computed using the data from Fig. 1). The enhanced helix stability at $D < D^*$ and $\lambda < 0.4$ can be explained using polymer arguments [17], from which it follows that when D is small enough the helical basin is entropically stabilized. Fig. 1 shows that the helical content of AS_3 and PN increases for all D. While for AS_2 and PA P_{HB} increases only below $D < D^* \sim (20 – 22)$ Å. The sequence-dependent values of D^* are difficult to predict using polymer theory alone. Interestingly, for AS_2 and PA we find that P_{HB} changes non-monotonically as D decreases (Figs. 1A and 1B). Such a behavior is also mirrored in the variation of R_{ee} as D is changed (data not shown), in agreement with theoretical predictions [34].

For small $\lambda(\sim 0.01)$, we expect that the effect of confinement can be described by the difference in entropy changes in the DSE and the HB. We estimate confinement-induced free energy changes using

$$\begin{aligned} \Delta\Delta G(D,\lambda\sim 0.01) &\approx -T[k_B ln(\alpha_{HB}(D)) - k_B ln(\alpha_{DSE}(D))] \\ &\approx -T[\Delta S_{HB}(D) - \Delta S_{DSE}(D)], \end{aligned} \quad (1)$$

where $\Delta S_{HB}(D)$ and $\Delta S_{DSE}(D)$ are the changes in entropy upon confinement of the helix and DSE, respectively. The volume fraction accessible to the HB ($\alpha_{HB}(D)$) and DSE ($\alpha_{DSE}(D)$),

are calculated numerically using the Widom particle insertion method (see SI for details). The similarity (Fig. 2) in the values of $\Delta\Delta G(D)$ computed using $\alpha_{HB}(D)$ and $\alpha_{DSE}(D)$ and that obtained directly from $P_{HB}(D)$ (Fig. 1) shows that the helix formed by AS_3 is entropically stabilized for all D. In contrast, $\Delta S_{DSE}(D) > \Delta S_{HB}(D)$ for AS_2 and PA when $D > D^* \sim 20$ Å which leads to destabilization of the helix upon confinement. Thus, the differences in the intrapeptide interaction strength between sequences AS_2 and AS_3 can change the nature of the DSE and HB, and can result in either helix stabilization (for AS_3) or helix destabilization (for AS_2) when $D > 20$ Å. The differing behavior of AS_2 ($\epsilon_{BB}/k_BT \approx 3$) and AS_3 ($\epsilon_{BB}/k_BT \approx 0.9$) shows that the nature of the conformations explored in the bulk affects confinement-induced stability. In principle, ϵ_{BB} can be altered in experiments by addition of cosolvents or by changing temperature.

Hydrophobic residues are pinned to the nanotube as λ increases

We expect that increasing λ should result in sequences containing hydrophobic residues to adsorb onto the nanotube wall. The probability density of finding a residue i at a distance r_i from the long nanotube axis, shows all sequences sample the interior of the nanotube at $\lambda = 0.01$ (Fig. 3). As a result, we expect that confinement-induced helix stabilization should be largely determined by entropy considerations. However, as λ increases, sequences containing hydrophobic residues (PA, AS_1, AS_2, and AS_3) can be pinned to the wall, as indicated by the greater probability density of peptide residues near the nanotube surface (Figs. 3A and 3B). In the case of the amphiphilic sequence, the peptide sticks to the wall (Fig. 3A) and forms a helix (Figs. 1A and 1C). The spatial distribution of residues in the HB corresponds well with the probability density plotted for $\lambda = 1.0$ (Fig. 3A). The results in Fig. 3, which show that hydrophobic residues are pinned to the wall, while polar residues are more likely to be sequestered in the interior of the nanotube, suggests that a 'phase separation' occurs on the molecular length scale between hydrophobic and polar peptide residues.

The distribution functions in Fig. 3 shows that for an amphiphilic sequence, the stability of helices should be determined by the opposing tendency of hydrophobic residues to be pinned to the wall of the nanotube and the preference of the polar residues to be localized in the interior. Indeed, we find that for AS_1, AS_2, and AS_3 the helical content increases as λ increases (Fig. 4). The effect of increasing λ is most dramatic for $AS_1(\epsilon_{BB} = 0)$, for which P_{HB} increases dramatically from below the bulk value of $P_{HB}^B \approx 0.17$ (Fig. 4A). For AS_1, the helix is greatly stabilized by the favorable interactions between the hydrophobic residues and the nanotube. In the case of AS_2, increasing λ maximizes the attractive interactions between B (hydrophobic) beads with the nanotube without compromising the intra-peptide BB interactions in the HB. Similarly, P_{HB} increases (Fig. 4B) for AS_3 ($\epsilon_{BB} = 0.5$ *kcal/mol*) as λ increases although the changes in P_{HB} occur over a wider range of λ compared to AS_2 ($\epsilon_{BB} = 2.125$ *kcal/mol*) (Fig. 4B).

When the amphiphilic sequence is in the HB, all of the hydrophobic residues are aligned on one side of the helix while the polar residues are exposed on the other side (Fig. 3A). Thus, for all variations of *AS* the HB is stabilized because it maximizes the hydrophobic interaction between the hydrophobic face of the helix and the hydrophobic surface of the nanotube. If the helical pitch (p) is commensurate with the distance between the carbon atoms (R_{CC}) along the long axis of the nanotube, we expect that the interactions between the hydrophobic residues and the nanotube can be maximized without compromising the helical structure. Conversely, if p and R_{CC} are incommensurate it is likely that the helix may be denatured. Thus, besides the sequence, the relative positions of the hydrophobic residues in the helix are also important determinants of stability in a nanotube, especially as λ increases.

Diagram of states of polyalanine in a carbon nanotube is rich

The interplay between the strength of the hydrophobic interactions and the entropy of confinement results in a rich phase diagram in the (λ, D) plane for PA (Fig. 5A). The stability of the HB decreases as λ increases as long as $D <\sim 20$ Å (see points 1, 5, and 6 in Fig. 5A). The effect is most dramatic in the narrowest tube (D = 14.9 Å in Fig. 5B) in which P_{HB} nearly vanishes as λ approaches unity. In larger nanotubes ($D > 20$ Å), P_{HB} increases by about (7-10)% as λ increases from $\lambda = 0.01$, reaches a maximum at $\lambda \sim 0.4$ and then decreases upon further increase in λ (Fig. 5B and see points 2, 3, and 4 in Fig. 5A). This modest helix stabilization occurs because the peptide weakly binds to the wall of the nanotube as λ increases (Figs. 3B and 5A, point 3), resulting in preferential alignment of the peptide along the long axis of the nanotube (Fig. 5B point 3 and Fig. 2A of the SI). At $\lambda \approx 0.4$ and $D > 20$ Å, the interaction with the nanotube is not strong enough to overcome the internal peptide energies which favor the helix. As a result, the nanotube-peptide interactions are maximized when the peptide is in the HB. As λ is further increased, hydrophobic interactions with the wall cause the helical content to decrease (Fig. 5B). In the largest nanotube ($D \approx 35$ Å), as λ approaches unity P_{HB} decreases because the peptide gets splayed out along the interior of the nanotube surface (Fig. 5A, point 4). For nanotubes with $D \approx 20$ Å, increasing λ stabilizes a 'broken' helix (Fig. 5, point 5) that does not align along the long nanotube axis (Fig. 2A in SI), but instead binds to the nanotube perpendicular to the nanotube axis (Fig. 2B in SI). For the smallest diameter nanotubes, increasing λ stabilizes a coiled peptide that coats the interior surface of the nanotube (Fig. 5A, point 6) but has no helical dihedral angles.

Taken together these results show that the effect of varying the hydrophobic character of the nanotube on helix stability is subtle for the PA. For the largest nanotube diameters there is an optimal hydrophobic strength which stabilizes the helix modestly. For smaller nanotube diameters divergent behavior is observed. Weakly hydrophobic nanotubes ($\lambda < 0.4$) stabilize the helix as D gets smaller. In contrast, destabilization of the helix occurs when $\lambda > 0.6$.

Hydrophobic patches lining the nanotube affect P_{HB} of PA

To mimic the chemical heterogeneity of the groups in the ribosome tunnel, which has small hydrophobic patches from proteins (such as L4, L17 and L39 in the ribosome of eukaryotes [4] surrounded by hydrophilic patches from RNA [35]), we created different size hydrophobic patches that line the nanotube (Fig. 6A). The desired heterogeneity is achieved by assigning hydrophilic character to subsets of nanotube atoms that run parallel to the long nanotube axis, and hydrophobic behavior to the rest of the nanotube atoms (see Methods section for details). With $\lambda = 0.9$, we vary the size of the hydrophobic patch. The fraction of hydrophobic surface area f_H varies from 0 to 1. Surprisingly, we find that the helical stability of PA, whose helical content is negligible at $\lambda = 0.9$ and $f_H = 1$ for all D (Fig. 1), increases as f_H decreases (Fig. 6B). In the smallest nanotube (D = 14.9 Å), P_{HB} increases monotonically as f_H decreases, with the smallest hydrophobic patch imparting the greatest helix stability. In larger nanotubes, P_{HB} as a function of f_H is nonmonotonic. Thus, there is an optimal f_H, between 0.08 and 0.15, in these larger nanotubes that maximizes P_{HB} for PA.

Conclusions

The effect of nanotube confinement on the stability of the helical states depends on the sequence, the tube diameter, nanotube-peptide interactions as well as the chemical heterogeneity of the the nanotube. The remarkably complex behavior of peptides in nanotubes illustrates that it is possible to control confinement-induced helix stability by altering a number of variables. The substantial diversity in the stability as a function of (D, λ), even for a specific sequence (Fig. 5A), shows that solvent-mediated peptide-nanotube interactions (parameterized by λ) can either stabilize or destabilize the HB depending on D. Our results show that it would

be erroneous to draw general conclusions [20] based on the study of a single sequence in a nanotube with various values of D.

A key prediction of this study is that confinement-induced helix stability can be dramatically altered by varying the intra-peptide interactions, or by changing the interaction strength between the peptide and the nanotube. The changes in the stability of the HB of the amphiphilic sequence (AS_1, AS_2, and AS_3) most vividly illustrate the effects of λ, ϵ_{BB}, and D (Fig. 1). The variations in ϵ_{HB} and ϵ_{BB}, which distinguish AS_1, AS_2, and AS_3, can be realized by varying cosolvent conditions. The differences in their stabilities upon confinement in AS_1, AS_2, and AS_3 is due to substantial changes in the DSE. The finding that the stability of a polyalanine sequence can be greatly altered by changing λ and D (see Fig. 5A) can be experimentally tested. The changes in λ can be achieved by varying the solvent density in the nanotube.

A prediction of plausible relevance to peptide folding in the ribosome is the demonstration that helix stability also depends strongly on the size of the hydrophobic patch lining the nanotube. If the entire interior of the nanotube is hydrophobic ($f_H = 1$), the HB of the polyalanine peptide is completely destabilized when the interaction between the peptide and the nanotube is $\lambda = 0.9$. However, as the patch takes up a smaller percentage of the surface area of the nanotube, the stability of the polyalanine helix increases. In the nanotube diameter range comparable to the ribosome tunnel ($D \approx 15$ Å), we find that the smallest size hydrophobic patches maximizes the helix stability. As a result, we predict that helix stability can increase in regions of the ribosome tunnel where small hydrophobic patches exist. Clearly, the extent of stabilization in the ribosome tunnel will depend on the sequence.

Supplementary Material

Refer to Web version on PubMed Central for supplementary material.

Acknowledgements

The authors thank Vincent Crespi for a computer program to generate atomic coordinates of carbon nanotubes. This work was supported in part by grants from the NSF (05-14056) to DT, Scientific Development Grant from the American Heart Association to GS, the Intramural Research Program of the NIH, National Heart Lung and Blood Institute to BRB, and a NIH GPP Biophysics Fellowship to EO.

References

1. Nissen P, Hansen J, Ban N, Moore PB, Steitz TA. Science 2000;289:920–929. [PubMed: 10937990]
2. Eggers DK, Valentine JS. Prot Sci 2001;10(2):250–261.
3. Thirumalai D, Lorimer GH. Ann Rev Biophys Biomol Struc 2001;30:245–269.
4. Woolhead CA, McCormick PJ, Johnson AE. Cell 2004;116(5):725–736. [PubMed: 15006354]
5. Groll M, Bochtler M, Brandstetter H, Clausen T, Huber R. Chembiochem 2005;6(2):222–256. [PubMed: 15678420]
6. Lu J, Deutsch C. Biochem 2005;44:8230–8243. [PubMed: 15938612]
7. Lu J, Deutsch C. Nat Struc Molec Biol 2005;12(12):1123–1129.
8. Hinnah SC, Wagner R, Sveshnikova R, Harrer R, Soll J. Biophys J 2002;83:899–911. [PubMed: 12124272]
9. Muro C, Grigoriev SM, Pietkiewicz D, Kinnally KW, Campo ML. Biophys J 2003;84:2981–2989. [PubMed: 12719229]
10. Hessa T, Kim H, Bihlmaier K, Lundin C, Boekel J, Anderson H, Nilsson I, White SH, voh Heijne G. Nature 2005;433:377–381. [PubMed: 15674282]
11. Mohammad MM, Prakash S, Matouschek A, Movileanu L. J Am Chem Soc 2008;130(12):4081–4088. [PubMed: 18321107]
12. Dekker C. Nat Nano 2007;2(4):209–215.

13. Betancourt MR, Thirumalai D. J Molec Biol 1999;287(3):627–644. [PubMed: 10092464]
14. Zhou HX, Dill KA. Biochemistry 2001;40(38):11289–11293. [PubMed: 11560476]
15. Klimov DK, Newfield D, Thirumalai D. Proc Natl Acad Sci USA 2002;99(12):8019–8024. [PubMed: 12060748]
16. Baumketner A, Jewett A, Shea JE. J Molec Biol 2003;332(3):701–713. [PubMed: 12963377]
17. Ziv G, Haran G, Thirumalai D. Proc Natl Acad Sci USA 2005;102(52):18956–18961. [PubMed: 16357202]
18. Cheung MS, Klimov D, Thirumalai D. Proc Natl Acad Sci USA 2005;102(13):4753–4758. [PubMed: 15781864]
19. Cheung MS, Thirumalai D. J Molec Biol 2006;357(2):632–643. [PubMed: 16427652]
20. Sorin EJ, Pande VS. J Am Chem Soc 2006;128(19):6316–6317. [PubMed: 16683786]
21. Elcock AH. PLOS Comp Biol 2006;2(7):824–841.
22. Minton AP. Biophys J 1992;63(4):1090–1100. [PubMed: 1420928]
23. Zhou HX. J Chem Phys 2007;127(24):245101. [PubMed: 18163710]
24. Degrado WF, Lear JD. J Am Chem Soc 1985;107:7684–7689.
25. Ho SP, Degrado WF. J Am Chem Soc 1987;109(22):6751–6758.
26. Xiong H, Buckwalter BL, Shieh HM, Hecht MH. Proc Natl Acad Sci USA 1995;92:6349–6353. [PubMed: 7603994]
27. Ziegler J, Sticht H, Marx UC, Muller W, Rosch P, Schwarzinger S. J Biol Chem 2003;278(50):50175–50181. [PubMed: 12952977]
28. Dima RI, Thirumalai D. Proc Natl Acad Sci USA 2004;101(43):15335–15340. [PubMed: 15494440]
29. Williams S, Causgrove TP, Gilmanshin R, Fang KS, Callender RH, Woodruff WH, Dyer RB. Biochemistry 1996;35(3):691–697. [PubMed: 8547249]
30. Kumar S, Bansal M. Biophys J 1998;75:1935–1944. [PubMed: 9746534]
31. Honeycutt JD, Thirumalai D. Proc Natl Acad Sci USA 1990;87:3526–3529. [PubMed: 2333297]
32. Veitshans T, Klimov D, Thirumalai D. Fold Des 1997;2(1):1–22. [PubMed: 9080195]
33. Brooks BR, Bruccoleri RE, Olafson BD, States DJ, Swaminathan S, Karplus M. J Comp Chem 1983;4:187–217.
34. Morrison G, Thirumalai D. J Chem Phys 2005;122:194907. [PubMed: 16161617]
35. Voss NR, Gerstein M, Steitz TA, Moore PB. J Molec Biol 2006;360:893–906. [PubMed: 16784753]
36. Guo Z, Thirumalai D. J Molec Biol 1996;263(2):323–343. [PubMed: 8913310]

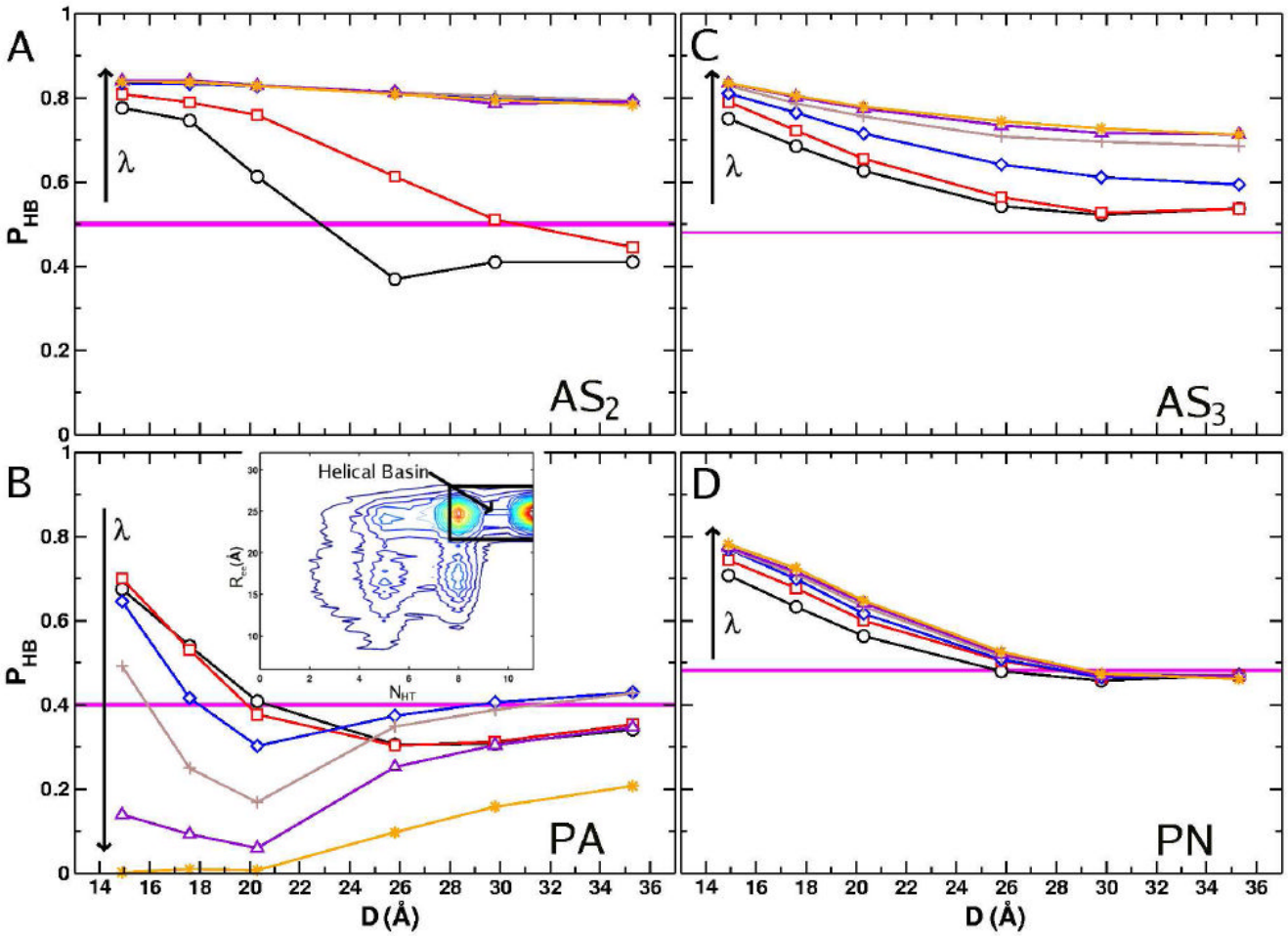

Figure 1.

The probability of being in the HB as a function of nanotube diameter for the sequences AS_2 (A), PA (B), AS_3 (C) and PN (D) at various λ values (λ= 0.01 (black circles), 0.1 (red squares), 0.3 (blue diamonds), 0.5 (brown plus signs), 0.7 (purple triangles) and 1.0 (orange stars)). The horizontal magenta colored line, in each graph, corresponds to the probability of being helical in bulk, and the width corresponds to the standard error of P_{HB}^{B}. We characterized a given peptide conformation as helical using two order parameters, the end-to-end distance (R_{ee}) and the number of backbone dihedral angles that are helical ('Helical Triads') (see the inset in (C)). A peptide conformation is helical if 21.25 Å < R_{ee} < 28.75 Å and $8 \leq N_{HT} \leq 11$.

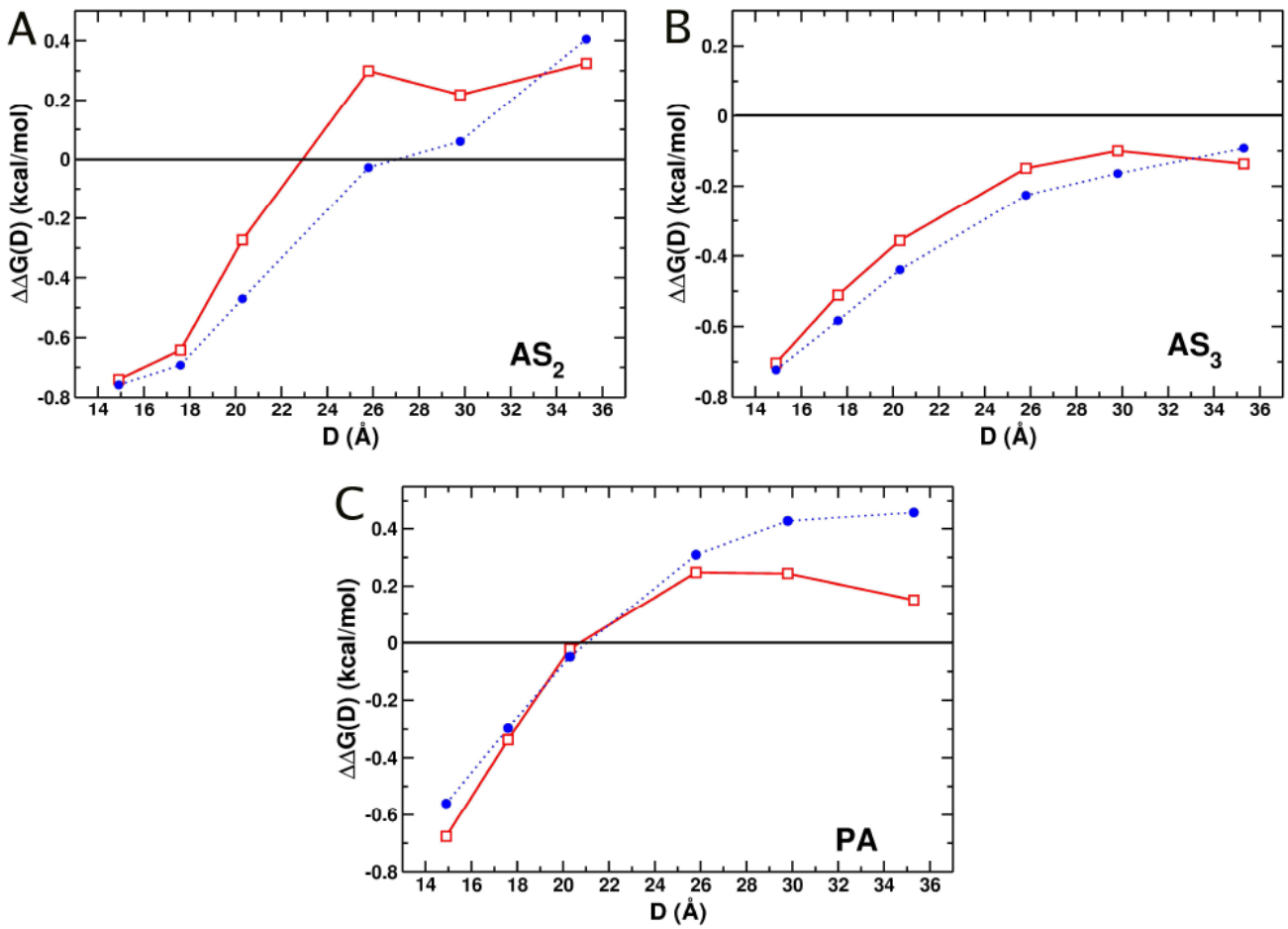

Figure 2.

The change in free energy ($\Delta\Delta G(D) = \Delta G(D) - \Delta G(B)$) of the HB, relative to the DSE, upon nanotube confinement as a function of D. The free energy difference in the bulk ($D \rightarrow \infty$) is given by $\Delta G(B)$. $\Delta\Delta G(D)$ computed from

$$P_{HB}(D)\,(\Delta\Delta G(D) = -k_B T \ln\left[\frac{P_{HB}(D)P_{HB}^{B}}{(1-P_{HB}(D))(1-P_{HB}^{B})}\right]$$

and $\alpha(D)$ (see Eq. 1) are shown as red squares and blue circles, respectively. Lines are to guide the eye. The results in panels (A), (B), and (C) are for AS_2, AS_3, and PA respectively.

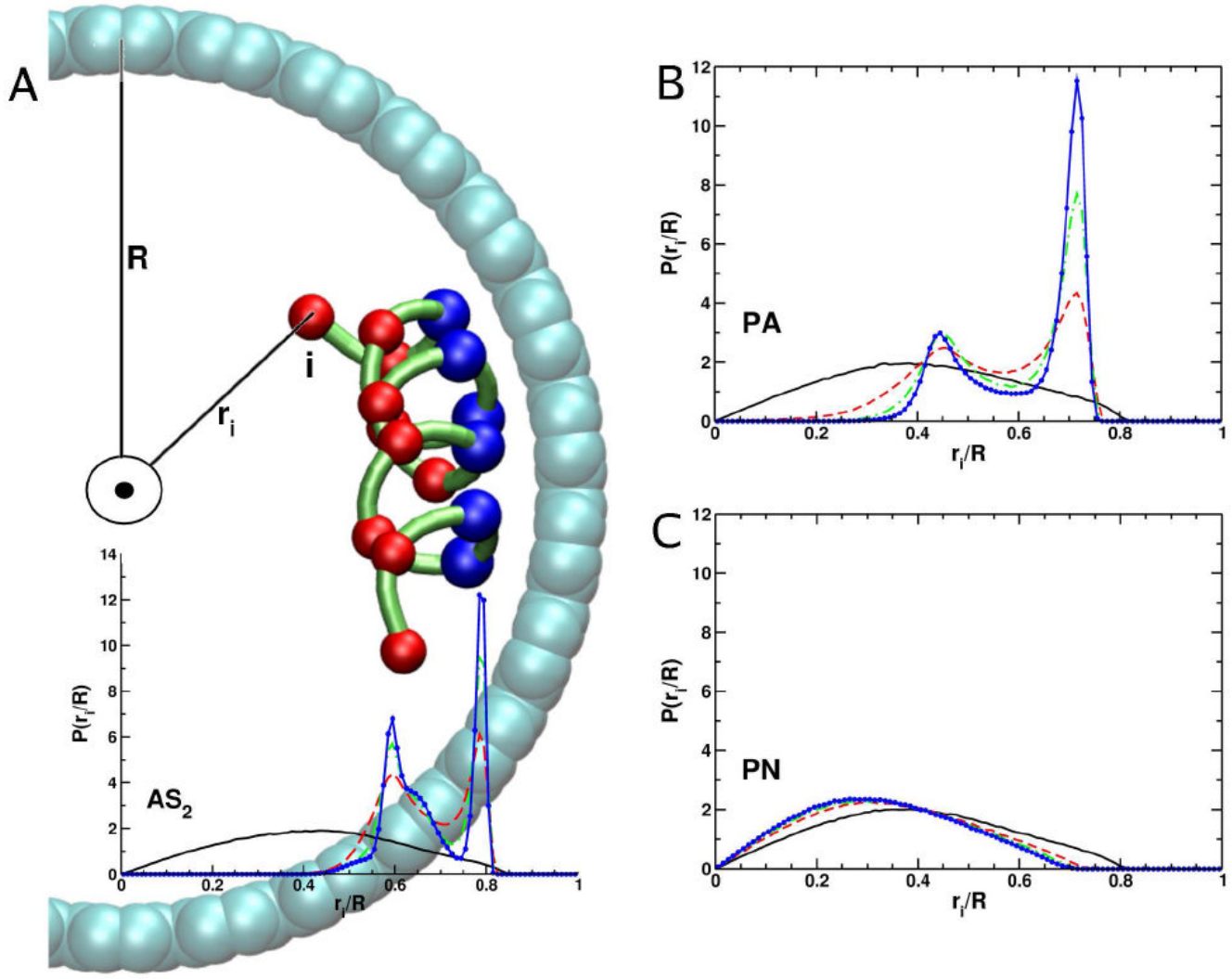

Figure 3.

The probability density of finding a residue *i* at a distance r_i/R (R, the nanotube radius, is 14.9 Å in (A), R = 12.9 Å in (B) and (C)) from the long nanotube axis at different λ values for AS_2 (A), PA (B) and PN (C). Four different values of λ are plotted, λ = 0.01 (solid black line), 0.3 (dashed red line), 0.7 (dash-dot green line) and 1.0 (solid blue line with circles). The image in the background of (A) is on the same scale as the graph overlaying it. The spatial distribution of the residues in the image correspond well with the probability density at λ = 1.0. In the image hydrophobic residues are shown in blue, and polar residues are in red.

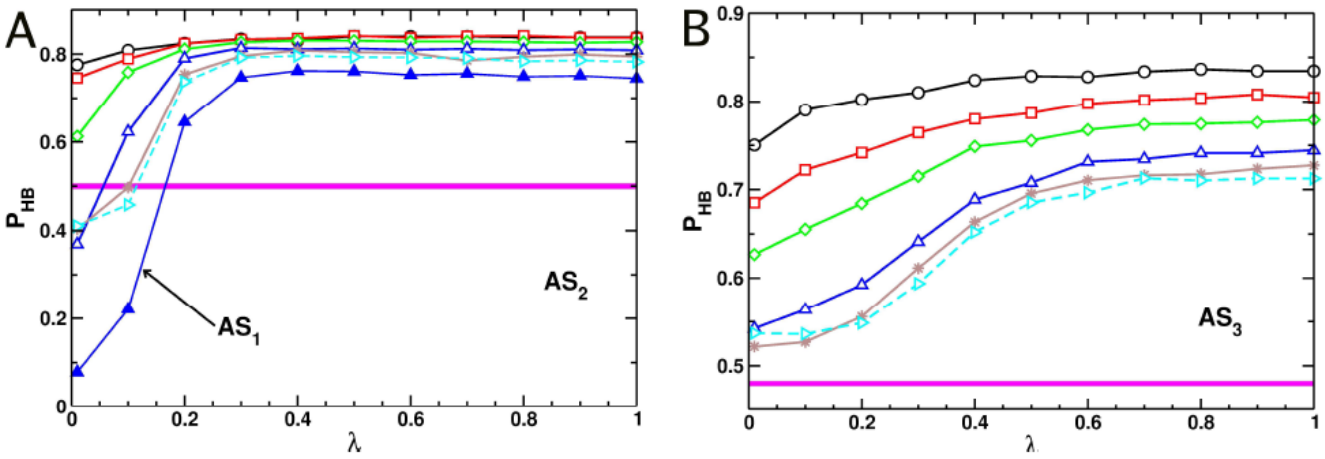

Figure 4.

Probability of being in the HB as a function of λ in different diameter nanotubes for the three variations of the amphiphilic sequence. The graphs show that AS_1, AS_2, and AS_3 tend to be stabilized by increasing the strength of the hydrophobic interactions with the nanotube. P_{HB} versus λ is shown for the two amphiphilic sequences AS_2 (A) and AS_3 (B) for different nanotube diameters (D = 35.3 Å - cyan triangles, 29.8 Å -brown stars, 25.8 Å - blue triangles, 20.3 Å - green diamonds, 17.6 Å - red squares, and 14.9 Å - black circles). Results for AS_1 with D = 25.8 Å are shown as blue filled triangles in (A).

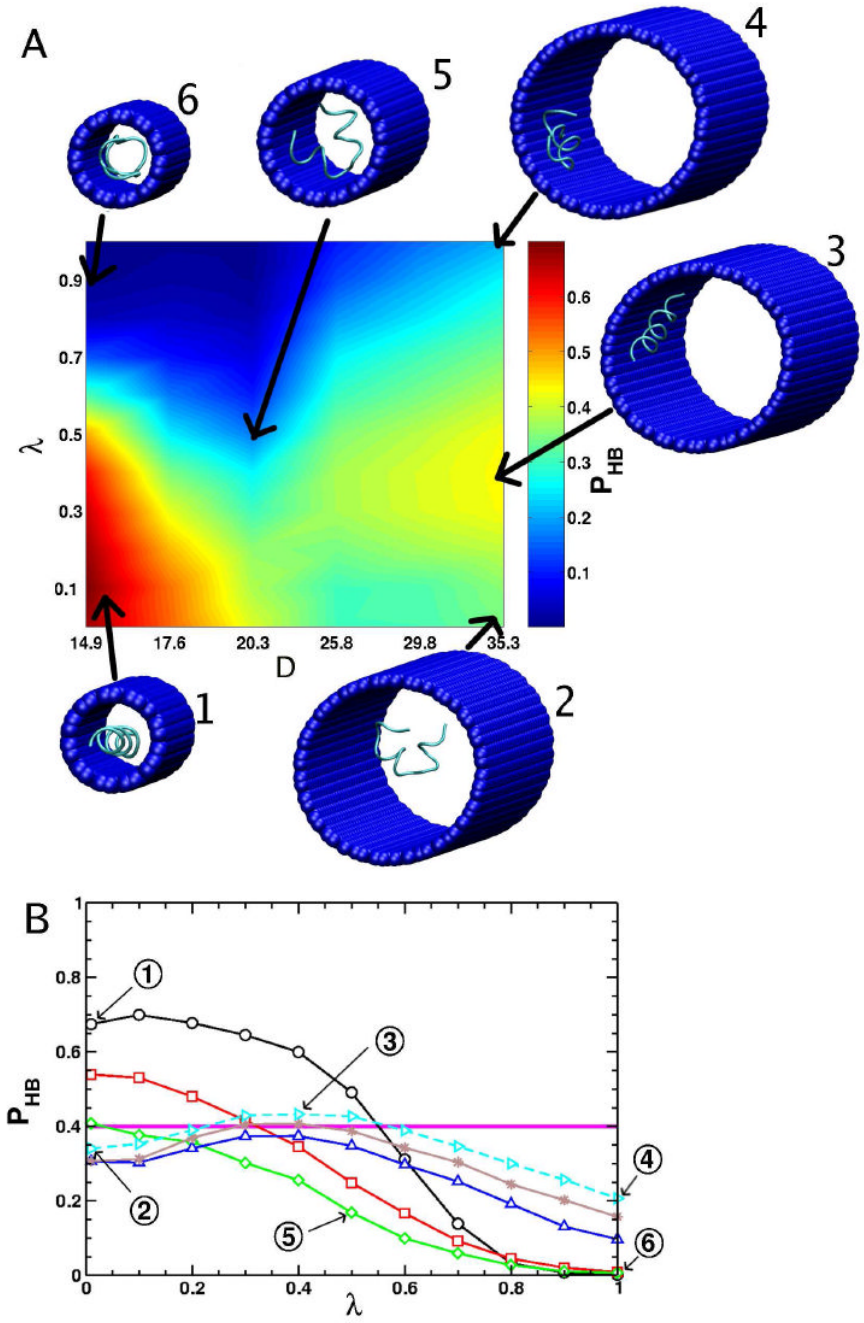

Figure 5.

The probability of being in the HB as a function of D and λ for PA. (A) Phase diagram in the (λ, D) plane. Representative structures are shown in the images labeled 1 through 6. (B) The dependence of P_{HB} on λ for various D. See Fig. 4 for explanation of the symbols. The points labeled 1 through 6 correspond to the structures labeled in (A).

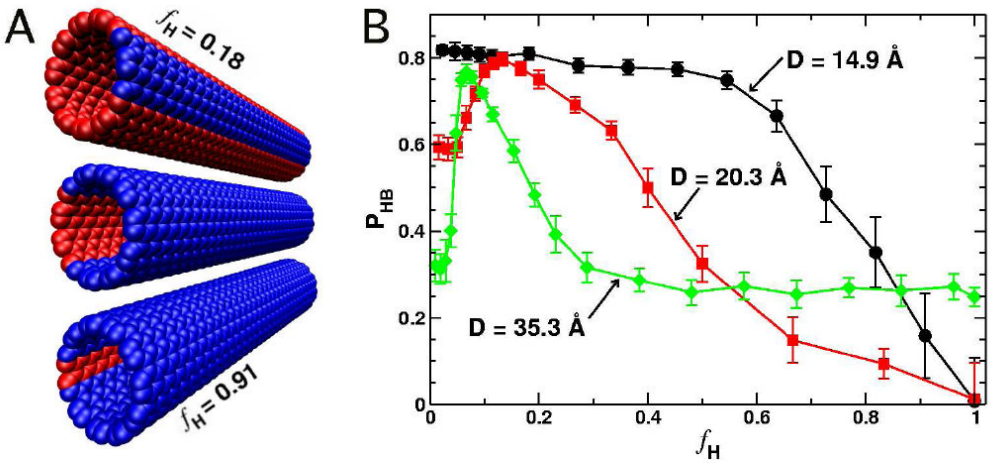

Figure 6.

Changes in P_{HB} in a chemically heterogeneous nanotube. (A) The size of the hydrophobic patch lining the nanotube (nanotube atoms with hydrophobic character are shown in blue, while those with hydrophilic character are shown in red). The value of D is 14.9 Å, and the fraction of nanotube hydrophobic surface area, f_H, is 0.18, 0.73 and 0.91 for the top, middle and bottom nanotubes. (B) The probability of being in the HB as a function of f_H with D = 14.9, 20.3 and 35.3 Å, and λ = 0.9. For the smallest nanotube, a homogeneous hydrophobic environment (f_H = 1) destabilizes the helix, while the smallest hydrophobic patches maximize helix stability. For larger D there is an optimal hydrophobic patch size that maximizes helix stability.

TABLE I

Models and simulation details

Sequence	Label	ϵ_{HB} [a]	ϵ_{BB} [b]	D (Å)	Time (μs) [c]	P_{HB}^{B} [d]
GDLDDLLKKLKDLLKG[e]	AS_1 [f]	0.00	2.125	25.8	2.0	0.17
	AS_2 [g]	1.75	2.125	all [h]	3.3	0.50
	AS_3 [i]	2.75	0.50	all	3.3	0.48
A_{16}	PA	2.75	0.50	all	3.3	0.40
N_{16}	PN	2.50	0.50	all	3.3	0.48

[a] The implicit hydrogen bonding energy in *kcal/mol*, see Eq. 6 in SI.

[b] The Lennard-Jones well-depth between hydrophobic residues in *kcal/mol*, see Eq. 5 in SI.

[c] The total simulation time per nanotube diameter.

[d] The probability of being in the HB in bulk.

[e] One letter code is used for amino acids.

[f] Original parameter set of Guo and Thirumalai [36].

[g] Modified Dihedral Potential (see Table 1 in SI) and V_{HB} term (see Eq. 6 in SI).

[h] 'all' indicates that nanotubes with D= 35.3, 29.8, 25.8, 20.3, 17.6, and 14.9 Å were studied.

[i] Same Parameter Set as AS_2 except ϵ_{BB} = 0.5 *kcal/mol*.